

Facile Solution Route to Vertically Aligned, Selective Growth of ZnO Nanostructure Arrays

Cheng Hung Wang,[†] Andrew See Weng Wong,[§] and Ghim Wei Ho^{*,†,‡}

Department of Electrical and Computer Engineering, 4 Engineering Drive, and Engineering Science Programme, 9 Engineering Drive 1, National University of Singapore, Singapore 117576, and Institute of Materials Research and Engineering, 3 Research Link, Singapore 117602

Received July 29, 2007. In Final Form: October 1, 2007

For any future cost-effective applications of inorganic nanostructures, in particular, hybrid photovoltaic cells, it is essential that these inorganic nanomaterials be solution processable and selectively printable. This letter reports the selective growth of single-crystal ZnO nanostructures based on the microcontact printing of an inorganic nanocrystal seeding film. The pattern-transfer quality is dependent on the concentration of the inking solution. Variable yet controllable anisotropic growth of ZnO nanowires has been demonstrated on the transferred patterns of ZnO nanocrystal films. The patterning and growth of these highly ordered arrays of ZnO nanostructures employ a simple soft lithography technique and mild reaction conditions at low temperature and in the absence of harmful organic additives.

1. Introduction

A revolutionary breakthrough in cutting costs and increasing the throughput of manufacturing photovoltaic and electronic devices can be achieved through reel-to-reel coating of materials from solution onto a large, flexible, light-weight platform. Thus, it is important to develop a low temperature, cheap, large-scale solution-based synthesis method and patterning of inorganic nanostructures because there is also great potential to synthesize these nanostructures on glass and plastic substrates for future flexible electronics and photovoltaic applications.

Recently, the patterning and self-assembly growth of nanostructures have received considerable attention. However, many of these methods require expensive equipment, multiple complex steps, and the use of photoresists and other harmful chemicals to obtain the selective growth of nanostructures whereas the new soft-lithography techniques can easily be employed for the large-scale patterning of any nanomaterial and biomaterial on the desired sites.^{1–3} Here we have looked into the solution-based growth of vertically aligned ZnO nanostructures on a selective area using a low-temperature, substrate-independent, environmental friendly method. This is done in line with our interest in fabricating hybrid photovoltaic cells. In previous cases, the photoactive layer of photovoltaic cells was made of a randomly interdispersed electron-accepting, hole-conducting polymer/inorganic material, where charge transport was limited by the hopping of electrons along the poorly connected network.^{4,5} To improve electron transport in these photovoltaic cells, arrays of 1D nanostructures infiltrated with inorganic material or conjugated polymers are designed to provide a direct path to the electrode.^{6–10} Therefore, it is apparent that the growth of highly ordered arrays of crystalline ZnO

nanostructures is necessary for efficient charge-transfer kinetics of photovoltaic cells. We have also noted that recently there have been many reports on the solution-based synthesis of ZnO nanostructures using Zn metal nitrate and acetate along with organic amine additives, namely, oleylamine, hexadecylamine, dioctylamine, dodecylamine, and methenamine.^{11–18} The commonly employed amine-mediated additives, which are nonpolar chelating agents, would preferentially attach to the nonpolar facets, thereby exposing the polar planes (*c* axis) for anisotropic growth.¹¹ However, in view of the environmental importance of eliminating harmful, corrosive organic additives in the synthesis process as well as in developing solvents in the patterning process, we have successfully developed a simple way to transfer patterns of ZnO nanocrystals onto various substrates and then use a facile solution-based synthesis to grow highly ordered ZnO nanostructures on selective areas.

2. Experimental Section

The poly(dimethylsiloxane) (PDMS) stamp was fabricated using Sylgard 184 silicone elastomer mixed with a curing agent (Dow Corning) in a ratio of 10:1 by weight. The silicone elastomer mixture was then cast on a photoresist-patterned Si master and evacuated in a vacuum jar. It was maintained at a pressure of 10⁻¹ Torr for 20 min to ensure that any trapped air bubbles were effectively removed. Finally, it was cured in a conventional oven at 60 °C for 24 h, and the PDMS stamp was peeled off of the master. The procedure for

(7) Takanezawa, K.; Hirota, K.; Wei, Q.-S.; Tajima, K.; Hashimoto, K. *J. Phys. Chem. C* **2007**, *111*, 7218–7223.

(8) Martinson, A. B. F.; McGarrah, J. E.; Parpia, M. O. K.; Hupp, J. T. *Phys. Chem. Chem. Phys.* **2006**, *8*, 4655–4659.

(9) Wei, Q.; Hirota, K.; Tajima, K.; Hashimoto, K. *Chem. Mater.* **2006**, *18*, 5080–5087.

(10) Peiro, A. M.; Ravirajan, P.; Govender, K.; Boyle, D. S.; O'Brien, P.; Bradley, D. D. C.; Nelson, J. J.; Durrant J. R. *J. Mat. Chem.* **2006**, *16*, 2088–2096.

(11) Sagunan, A.; Warad, H. C.; Boman, M.; Dutta, J. *J. Sol. Gel Sci. Techn.* **2006**, *39*, 49–56.

(12) Zhang, Z.; Lu, M.; Xu, H.; Chin, W.-S. *Chem. A. European Journal* **2006**, *13*, 632–638.

(13) Hambrook, J.; Rabe, S.; Merz, K.; Birkner, A.; Wohlfart, A.; Fischer, R. A.; Driess, M. *J. Mater. Chem.* **2003**, *13*, 1731–1736.

(14) Vayssieres, L. *Adv. Mater.* **2003**, *15*, 464–466.

(15) Greene, L. E.; Law, M.; Goldberger, J.; Kim, F.; Johnson, J. C.; Zhang, Y.; Saykally, R. J.; Yang, P. *Angew. Chem., Int. Ed.* **2003**, *42*, 3031–3034.

(16) Cross, R. B. M.; De Souza, M. M.; Narayanan, E. M. S. *Nanotechnology* **2005**, *16*, 2188–2192.

(17) Lin, Y.-R.; Yang, S.-S.; Tsai, S.-Y.; Hsu, H.-C.; Wu, S.-T.; Chen, I.-C. *Cryst. Growth Des.* **2006**, *6*, 1951–1955.

(18) Hu, C. H.; Wu, J. J. *J. Phys. Chem. B* **2006**, *110*, 12981–12985.

* Corresponding author. E-mail: esphgw@nus.edu.sg / elehgw@nus.edu.sg.

[†] Department of Electrical and Computer Engineering, National University of Singapore.

[‡] Engineering Science Programme, National University of Singapore.

[§] Institute of Materials Research and Engineering.

(1) Bernard, A.; Delamarche, E.; Schmid, H.; Michel, B.; Bosshard, H. R.; Biebuyck, H. *Langmuir* **1998**, *14*, 2225–2229.

(2) Bernard, A.; Rernard, J. P.; Renault, J. P.; Michel, B.; Bosshard, H. R.; Delamarche, E. *Adv. Mat.* **2000**, *12*, 1067–1070.

(3) Meitl, M. A.; Zhou, Y.; Gaur, A.; Jeon, S.; Usrey, M. L.; Strano, M. S.; Rogers, J. A. *Nano. Lett.* **2004**, *4*, 1643–1647.

(4) Bassler, H. *Mol. Cryst. Liq. Cryst. Sci. Technol.* **1994**, *252*, 11–21.

(5) Kang, Y.; Park, N.-G.; Kim, D. *Appl. Phys. Lett.* **2005**, *86*, 113101–113103.

(6) Law, M.; Greene, L. E.; Johnson, J. C.; Saykally, R.; Yang, P. *Nature Mat.* **2005**, *4*, 455–459.

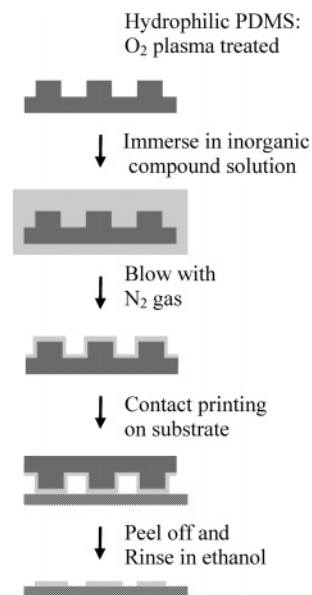


Figure 1. Schematic diagram of the microcontact printing process of the inorganic compound solution on a clean substrate.

the printing is shown schematically in Figure 1. The patterned PDMS stamps were cleaned in isopropyl alcohol, ethanol, and deionized water before O_2 plasma oxidation to create hydrophilic surfaces. The PDMS stamp was immersed in a 5–10 mM aqueous zinc acetate dihydrate ($Zn(C_2H_3O_2)_2 \cdot 2H_2O$) solution for 10 min, blown dried with N_2 gas, and stamped onto clean substrates (glass, plastics, and Si) for 10 min. The substrates were then rinsed in clean ethanol, blown dried with N_2 gas, and annealed in a furnace at 200–350 °C for 30 min. Subsequently, the growth of the ZnO nanowires was carried out using aqueous zinc acetate dihydrate without using any organic additives. The growth took place in a tight polypropylene screw cap where the printed substrates were placed. The bottles were heated in an oven at a relatively low temperature of 85–90 °C for 5–8 h. Finally, the products were washed with distilled water to remove any residual salts and organic material and then dried at 100 °C for at least 60 min. The crystal structures of the as-synthesized nanostructures were analyzed using transmission electron microscopy (TEM, Phillips FEG CM300) and X-ray diffractometry (XRD, Philip X-ray diffractometer equipped with graphite-monochromated $Cu K\alpha$ radiation at $\lambda = 1.541 \text{ \AA}$). The morphologies were characterized using scanning electron microscopy (SEM, JEOL FEG JSM 6700 F, secondary electron imaging) and atomic force microscopy (AFM, Digital Instruments). Photoluminescence (PL) properties were measured using a Rapid Photoluminescence Mapping Accent rpm 2000 He–Cd laser at 325 nm and 1.8 mW.

3. Results and Discussion

The PDMS stampings of inking solution (aqueous zinc acetate dihydrate) concentrations of 20, 5, and 1 mM were carried out on various substrates. AFM was used to map the topography of the transfer-printed and postannealed films on the Si substrate (Figure 2a–c). We have found that the concentration of the inking solution plays an important role in the success of pattern transfer because such low-density ZnO nanocrystals were transferred onto the Si surface at relatively low concentration (1 mM) (Figure 2a) whereas dense, agglomerated ZnO nanocrystals were transferred at high concentration (20 mM) (Figure 2c). However, at a concentration of 5–10 mM, we have observed that the transferred, postannealed film was uniformly covered with quasi-spherical nanocrystals (Figure 2b). The average diameter of the microprinted nanocrystals (ca. 5 nm) was determined from the height profile rather than the surface topography (Figure 2d) because of the poor lateral resolution of tip-shaped convolution. Figure 2e shows the 2D XRD Debye diffraction pattern obtained

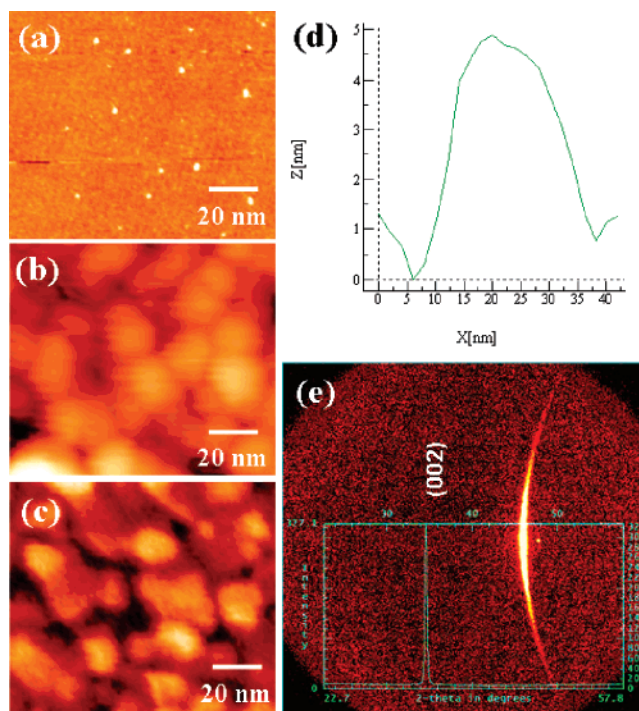


Figure 2. (a–c) AFM topographic images of microcontact-printed ZnO nanocrystals of various inking concentrations: 1, 5, and 20 mM, respectively. (d) Height profile analysis of the 5 mM ZnO nanocrystal film. (e) Two-dimensional XRD Debye pattern showing the c -axis (002) texturing of the wurtzite ZnO structure.

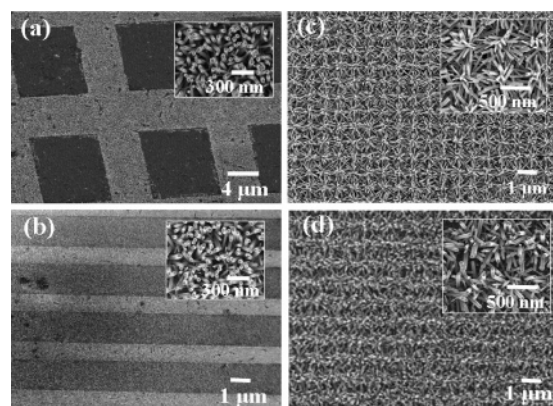


Figure 3. SEM images of ZnO nanowires grown on various periodicity patterns of approximately (a) 5 μm lines and 10 μm spacing, (b) 1 μm lines and 1.5 μm spacing, and (c, d) 0.5 μm lines and spacing.

on the postannealed nanocrystal film. A high intensity, nondispersive Debye ring shows only the existence of a ZnO(002) plane, which indicates that complete c -axis textured alignment has occurred on the film. This result complements the XRD pattern (Figure 2e), where a sharp, narrow fwhm peak at $2\theta = 34.4^\circ$ attributed to the ZnO(002) crystal plane (lattice constant of 5.206 \AA) was observed.¹⁷ This is not surprising because it has been reported that zinc acetate decomposition starts at $\sim 235^\circ\text{C}$ and converts completely to ZnO from 300 to 350 °C on the basis of differential thermal analysis and thermogravimetric analysis.¹⁹

Figure 3 shows the SEM images of ZnO nanowires grown on the postannealed ZnO nanocrystals films (Si substrates) of 1 mM inking concentration. Figure 3a,b shows the ZnO nanowires grown on different periodicity patterns with lines of 1–5 μm and

(19) Wei, M.; Zhi, D.; Driscoll, J. L. M. *Nanotechnology* **2005**, *16*, 1364–1368.

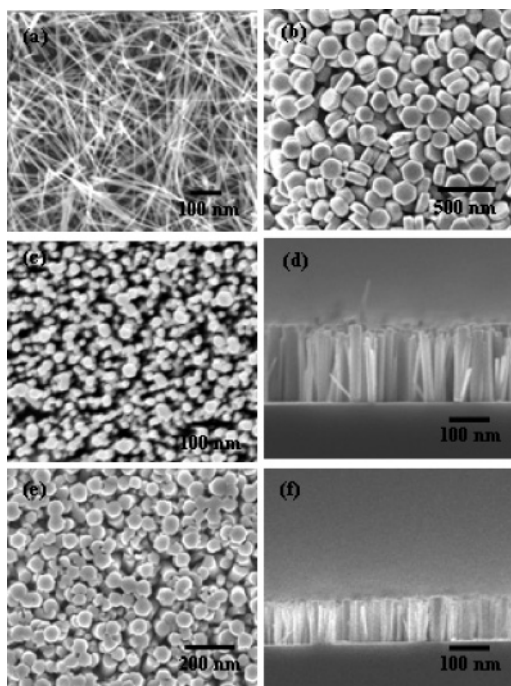


Figure 4. Top and cross-sectional SEM images of ZnO nanostructures grown at different zinc acetate concentration: (a) 1 mM, (b) 0.1 M, (c, d) 5 mM, and (e, f) 50 mM.

spacing of 1–10 μm at a precursor concentration of 10 mM and a temperature of 85 $^{\circ}\text{C}$ for a period of 8 h. It is apparent that the nanowires were selectively grown on only the patterned regions, and at higher magnification (Figure 3a,b insets), vertically aligned nanowires are observed to have diameters of ~ 50 –100 nm and lengths of ~ 100 –200 nm. It is also noted that the nanowires grown at the edge of the patterns are less aligned because of the edge printing effect phenomenon.²⁰ This phenomenon, whereby excess nanocrystals are printed mainly at the edges, becomes more pronounced when the periodicity of the pattern is $< 0.5 \mu\text{m}$. From Figure 3c,d (periodicity line pattern and spacing of 0.5 μm), it is seen that the nanowires that are grown radiate outward instead of being vertically aligned. The edge printing effect is believed to be closely related to the rough-edge structures of the pattern stamp and the weak interaction between the nanocrystals and the stamp.²⁰ Because of the weak interaction and rough surfaces edges, the nanocrystals aggregated at the pattern edges during N_2 drying and were then transferred onto substrates.²⁰ At the present moment, we are still working on controlling the edge printing effect to improve the alignment and selective growth of ZnO nanostructures for smaller periodicity patterns. However, in general most of the larger periodicity ($> 1 \mu\text{m}$) PDMS stamp patterns were successfully printed and transferred onto substrates, regardless of the shape of the pattern on the PDMS stamps. The stamps can effectively be reused many times without any significant deterioration.

Moving on to the discussion on the growth of ZnO nanostructures on preprinted ZnO nanocrystals films, we have found that the variation of the zinc acetate precursor concentration is an important factor in controlling the dimensions of the ZnO nanostructures grown on the substrates. This additive-free synthesis method shown here has successfully synthesized bundles of high-aspect-ratio ZnO nanowires prepared using 1 mM zinc acetate (Figure 4a). Individual long, thin ZnO nanowires have an average diameter of ~ 20 nm and a length of $\sim 2 \mu\text{m}$. As the zinc acetate concentration is drastically increased to 0.1 M, it is observed that the 1D nanostructures have transformed into 3D

monodisperse hexagonal ZnO crystals of ~ 250 nm diameter (Figure 4b). However, when the zinc acetate concentration is decreased to 5 mM, vertically aligned, discrete nanowires of 30–60 nm diameter and ~ 200 nm length are produced (Figure 4c). It is noted that at a controlled intermediate concentration the synthesized nanostructures are no longer randomly aligned as evidently shown by the cross-sectional SEM image of Figure 4d. At a 10-fold increase in zinc acetate concentration to 50 mM, it is observed that the average diameter of the nanowires has increased to ~ 100 nm and exhibits a quasi-hexagonal nanostructure (Figure 4e) whereas the cross-sectional SEM image (Figure 4f) still shows vertically aligned structures of ~ 100 nm height. For ordered solar cell architecture, small-diameter nanowires and closely spaced neighboring nanowires are necessary to ensure high, efficient charge separation.^{21–22} We expect that with the control of the ZnO nanocrystals' seeding layers and growth reaction parameters, the gap separation and the density of the ZnO nanowires can be tailored accordingly.

We have reasoned that the presence of a preprinted seeding nanocrystals film has facilitated the growth and orientation of ZnO nanowires. Deionized water acts as a nucleophilic reactant that leads to the hydrolysis and polymerization of the zinc acetate complexes to form zinc hydroxide clusters.²³ Zinc hydroxide embryonic clusters grew into nuclei on the seeded substrates by heterogeneous nucleation, which then transformed into zinc oxide. It is known that zinc hydroxide undergoes decomposition reactions to form zinc oxide ($\text{Zn}(\text{OH})_2 \rightarrow \text{ZnO} + \text{H}_2\text{O}$) from 70 to 140 $^{\circ}\text{C}$.²⁴ The growth of the ZnO nanostructures involves the mass transport and nucleation of solute from bulk zinc acetate dihydrate solution onto the nanocrystals film driven by the solute concentration gradient. The designated growth morphology is determined by the initial degree of supersaturation. When the solute concentration is relatively low (1 mM), the growth of randomly aligned bundles of ZnO nanowires is observed. These small but highly uniform diameter nanowires tend to bundle and align in the same growth direction and can be described by the phenomena of multiplication growth through the oriented attachment process.²⁵ However, at an intermediate concentration (≥ 5 mM), aligned growth of the ZnO nanowires on the seeded substrate becomes predominant. A further increase in concentration to 0.1 M gives a very supersaturated solution, whereby the homogeneous nucleation and growth of ZnO structures within the bulk solution become predominant. At this point, the homogeneous nucleation becomes evident because white precipitates are visibly observed in the reaction solution itself. The very supersaturated solution leads to the formation of well-developed 3D hexagonal structures. Thus, a clear correlation can be derived between the aspect ratio (length/diameter) and the zinc acetate concentration, and as such, they are inversely related.

Figure 5a shows a low-resolution image of nanowires that were dispersed on a holey carbon–copper grid. High-resolution TEM observation (Figure 5b) reveals single-crystal structures with lattice spacing of ~ 0.52 nm perpendicular to the longitudinal axis direction of the nanowire. This corresponds to the growth direction of [002] *c*-axis hexagonal ZnO.²⁶ According to the

(20) Wu, X. C.; Lenhart, S.; Chi, L. F.; Fuchs, H. *Langmuir* **2006**, *22*, 7807–7811.

(21) Savenije, T. J.; Warman, J. M.; Goossens, A. *Chem. Phys. Lett.* **1998**, *287*, 148–153.

(22) Arango, A. C.; Johnson, L. R.; Bliznyuk, V. N.; Schlesinger, Z.; Carter, S. A.; Horhold, H. H. *Adv. Mater.* **2000**, *12*, 1689–1692.

(23) Pierre, A. C. *Introduction to Sol-Gel Processing*; Kluwer Academic Press: Boston, 1998.

(24) Govender, K.; Boyle, D. S.; Kenway, P. B.; O'Brien, P. *J. Mat. Chem.* **2004**, *14*, 2575–2591.

(25) Banfield, T. F.; Welch, S. A.; Zhang, H.; Ebert, T. T.; Penn, R. L. *Science* **2000**, *289*, 751–754.

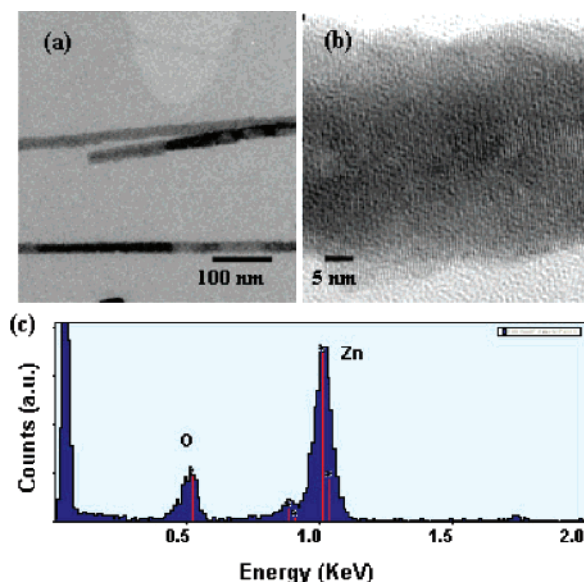


Figure 5. TEM structural characterization of nanowires dispersed on a holey carbon grid. (a) Low-resolution (b) high-resolution images and (c) TEM-EDX spectrum of the as-produced nanowire with 1:1 Zn/O.

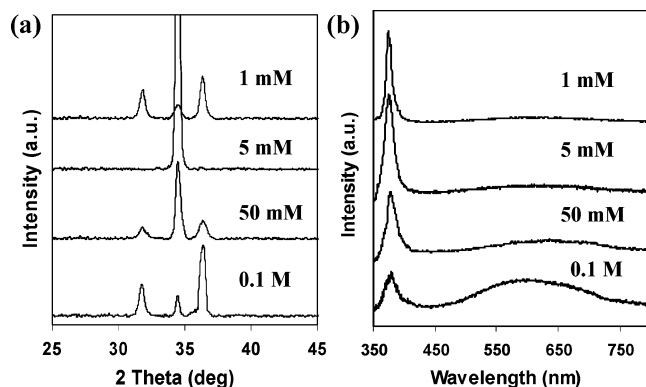


Figure 6. (a) XRD patterns and (b) PL spectra of ZnO nanostructures prepared at various concentrations. The enhanced (002) XRD diffraction peaks indicate the oriented growth of ZnO nanorod arrays. The quenching of UV emission may suggest an increase in the structural defect density.

TEM energy dispersive X-ray (EDX) analysis shown in Figure 5c, the atomic ratio of Zn and O in the nanowire is 0.51:0.49, which confirms the chemical composition and stoichiometry of ZnO nanowires. Figure 6a shows the XRD patterns of the hydrothermally prepared ZnO nanostructures. All of the diffraction peaks can be indexed to wurtzite-structured ZnO (JCPDS card no. 3-1451) with no traces of impurities.²⁷ The relative peak intensities are different from those of the standard powder diffraction of bulk ZnO, which can be explained by the preferential growth or alignment of the synthesized ZnO nanostructures. XRD patterns obtained from the 5 and 50 mM samples show strong peaks at $2\theta = 34.4^\circ$ attributed to the ZnO(002) crystal plane with a lattice constant of 5.206 Å. The enhanced (002) diffraction peaks of the 50 and 5 mM samples are consistent with the SEM images that show the oriented growth of ZnO nanowire arrays along the *c* axes.¹⁷ The fwhm of the diffraction peaks are small, which indicates the high crystal quality of the synthesized nanostructures. However, XRD patterns obtained from 1 and 0.1 M samples do not show any preferential alignment.

Figure 6b shows the room-temperature PL spectra obtained from the ZnO nanostructures. In general, ZnO PL spectra are

made up of two band emissions—the ultraviolet band emission (380 nm) and the visible light band emission (640 nm).^{17,28} The strong UV emission is attributed to the radiative recombination of electrons in the conduction band and holes in the valence band²⁹ whereas the visible emission is attributed to various intrinsic defects such as antisite oxygen defects, donor–acceptor complexes, and interstitial zinc.^{30–31} The intensity of the visible emission is a function of the defects, which is affected by the synthesis process as well as the dimensions of the ZnO nanostructures.³² Hence, the intensity of the visible-to-UV emission can be a measure of the quality of the produced ZnO nanostructures.³² The PL spectra were obtained from the ZnO nanostructures grown with various Zn acetate reagent concentrations. A comparison of all spectra shows that the relatively higher aspect ratio nanostructures display sharp emissions at ~ 380 nm with a narrow fwhm of 15–20 nm whereas the commonly observed visible defect peak is absent. As the aspect ratio of the nanostructures decreases, the quenching of the visible emission is no longer observed. The UV-to-visible emission ratio progressively decreases with the aspect ratio of the ZnO nanostructures, which may point to the fact that the ZnO defect density may vary with dimensions. In addition, the ZnO PL properties are also affected by the synthesis process because we have also carried out PL measurements on comparative nanostructure dimensions as produced by the zinc nitrate reagent,³³ which indicates a higher crystal defect density than for the Zn acetate-produced nanostructures. Thus, the present synthetic method has demonstrated a high UV-to-visible emission, which suggests a significant reduction in structural defects. In-depth investigations will be carried out to identify the types of defects that are responsible for the observed emissions.

4. Conclusions

We have demonstrated the selective growth of ordered single-crystal ZnO nanostructures based on the microcontact printing of nanocrystal seeding films. The pattern-transfer quality is dependent on the concentration of the inking solution. The optimized concentration of the inking solution is 5 mM because the transferred and postannealed film is uniformly covered with nanocrystals. We have also shown that variable yet controllable anisotropic growth of ZnO nanostructures can be carried out without using an organic-assisted capping reagent. The produced ZnO nanostructures are of high structural quality, exhibiting single crystals, low intrinsic defects, and high UV emission. The success of the patterning and growth of these inorganic nanostructures employs a simple soft lithography technique and mild reaction conditions—low temperatures and no harmful organic additives. Finally, we expect that with good control of the ZnO nanocrystal seeding layers and reaction parameters, the dimension, gap separation, and the density of the ZnO nanowires can be tailored for various applications.

Acknowledgment. We acknowledge the financial support of the National University of Singapore, research grant R-533 000 002 123.

LA702296Q

(26) Liou, S.-C.; Hsiao, C.-S.; Chen, S.-Y. *J. Cryst. Growth* **2005**, *274*, 438–446.

(27) Guo, M.; Diao, P.; Cai, S. J. *Solid State Chem.* **2005**, *178*, 1864–1873.

(28) Qian, H. S.; Yu, S. H.; Gong, J. Y.; Luo, L. B.; Wen, L. L. *Cryst. Growth Des.* **2005**, *5*, 935–939.

(29) Gao, X.; Li, X.; Yu, W. *J. Phys. Chem. B* **2005**, *109*, 1155–1161.

(30) Wang, D.; Song, C. J. *Phys. Chem. B* **2005**, *109*, 12697–12700.

(31) Gomi, M.; Oohira, N.; Ozaki, K.; Koyano, M. *Jpn. J. Appl. Phys.* **2003**, *42*, 481–485.

(32) Chen, J.; Fujita, T. *Jpn. J. Appl. Phys.* **2003**, *42*, 602–606.

(33) Ho, G. W.; Wong, A. S. W. *Appl. Phys. A* **2007**, *86*, 457–462.